An optimal control approach of integrating traffic signals and cooperative vehicle trajectories at intersections

Liu, Meiqi; Zhao, J.; Hoogendoorn, S. P.; Wang, M.

DOI
10.1080/21680566.2021.1991505

Publication date
2021

Document Version
Final published version

Published in
Transportmetrica B

Transportmetrica B: Transport Dynamics

ISSN: (Print) (Online) Journal homepage: https://www.tandfonline.com/loi/ttrb20

An optimal control approach of integrating traffic signals and cooperative vehicle trajectories at intersections

Meiqi Liu, J. Zhao, S. P. Hoogendoorn & M. Wang

To cite this article: Meiqi Liu, J. Zhao, S. P. Hoogendoorn & M. Wang (2021): An optimal control approach of integrating traffic signals and cooperative vehicle trajectories at intersections, Transportmetrica B: Transport Dynamics, DOI: 10.1080/21680566.2021.1991505

To link to this article: https://doi.org/10.1080/21680566.2021.1991505

Published online: 21 Oct 2021.

TRANSPORTMETRICA B: TRANSPORT DYNAMICS
https://doi.org/10.1080/21680566.2021.1991505

Taylor & Francis
Taylor & Francis Group

An optimal control approach of integrating traffic signals and cooperative vehicle trajectories at intersections

Meiqi Liu[a], J. Zhao [b], S. P. Hoogendoorn [a] and M. Wang[a]

[a]Department of Transport & Planning, Delft University of Technology, Delft, The Netherlands; [b]Department of Traffic Engineering, University of Shanghai for Science and Technology, Shanghai, People's Republic of China

ABSTRACT

An integrated approach for optimising traffic signals and cooperative vehicle trajectories at urban intersections is proposed. The upper layer determines the optimal signals using enumeration and the lower layer optimises trajectories under each feasible signal plan. In the lower layer, platoon accelerations are optimised considering comfort and delay while satisfying motion constraints and safe requirements. The red phase is enforced as a logic constraint, which restricts vehicles to stay behind the stop-line. Typical platoon manoeuvres such as split and approach can be included in the lower layer. The integrated control approach is adaptive to traffic demands and flexible in incorporating different traffic movements during multiple signal phases. The controller performance is verified by simulation of three designed scenarios. The comparison with trajectory optimization and signal optimization demonstrates the advantages on throughput, fuel economy, delay and vehicle stops, and reveals insights into the optimal patterns on signals and trajectories.

ARTICLE HISTORY
Received 8 January 2021
Accepted 3 October 2021

KEYWORDS
Trajectory planning; signalised intersections; optimal control; cooperative vehicles

1. Introduction

The suboptimal setting of traffic lights is considered to be one of the leading causes of travel delay as well as excessive fuel consumption and emissions on urban roads (Ubiergo and Jin 2016). Considerable numbers of studies have been conducted to relieve this problem at urban intersections from design, control, and management perspectives (Zhao, Knoop, and Wang 2020; Guler, Menendez, and Meier 2014). Connected and automated vehicle (CAV) technology enables the roadside infrastructure to communicate with the onboard vehicle control algorithms (Wang et al. 2014). The promise of further optimising traffic conditions has led to a surge in the number of studies devoted to enhancing traffic operations at signalised intersections by the improved and integrated design of traffic signals and/or CAV trajectories.

Four directions have been explored with respect to CAV platooning at urban intersections, i.e. cooperative intersection systems, speed advisory algorithms, CAV trajectory planning and the optimisation of traffic signals and vehicle trajectories. The cooperative intersection algorithms develop a signal-free intersection to coordinate CAVs departing the intersection without collision (Lee and Park 2012; Ahmane et al. 2013; Lee, Park, and Yun 2013; Zohdy and Rakha 2016; Yu et al. 2019), but the challenges of this line of research are how to consider the safety requirements of pedestrians and cyclists. Speed advisory systems such as GLOSA (Green Light Optimised Speed Advisory) (Stevanovic, Stevanovic, and

CONTACT Meiqi Liu Meiqi.Liu@tudelft.nl Department of Transport & Planning, Delft University of Technology, Delft, The Netherlands

Kergaye 2013; Li, Dridi, and El-Moudni 2014; Stebbins et al. 2017) and Eco-Approach and Departure systems (Altan et al. 2017; Hao et al. 2018; Wang, Wu, and Barth 2019), aim at providing speed advice to avoid stops when passing signalised intersections, causing fewer stops and energy consumptions. However, only individual vehicles are considered in these systems, neglecting the benefits of operating the overall vehicle platoons. CAV trajectory planning systems optimise vehicle trajectories at isolated intersections (Zhao et al. 2018; Jiang et al. 2017) or along a corridor (Asadi and Vahidi 2010; Kamal et al. 2012; He, Liu, and Liu 2015; Wan, Vahidi, and Luckow 2016; HomChaudhuri, Vahidi, and Pisu 2017; Liu, Wang, and Hoogendoorn 2019), whereas the signal phase and timing information is used as exogenous inputs to the optimisation problem and consequently the superiority of integrated information between vehicles (i.e. speed and position) and infrastructures (i.e. signal parameters) is hampered for lack of signal optimisation.

The integrated approaches of optimising traffic signals and vehicle trajectories in (Li, Elefteriadou, and Ranka 2014; Yang, Guler, and Menendez 2016; Xu et al. 2018; Feng, Yu, and Liu 2018; Guo et al. 2019) generally adopt a two-layered structure to solve the problem. In the signal optimisation layer, the enumeration method (Li, Elefteriadou, and Ranka 2014; Xu et al. 2018) and the similar forward/backward recursion method (Feng, Yu, and Liu 2018; Guo et al. 2019) are applied, whereas the signals are not explicitly optimised in a few studies (Li, Elefteriadou, and Ranka 2014; Yang, Guler, and Menendez 2016; Yu et al. 2018). The red phase in the signal layer is considered as constraining the arrival time in (Guo et al. 2019; Feng, Yu, and Liu 2018; Xu et al. 2018), which requires estimation of vehicle arrival time at the stop bar. In the vehicle trajectory layer, as opposed to trajectory optimisation of the whole platoon, the platoon leader trajectories (Feng, Yu, and Liu 2018; Yu et al. 2018) or the individual vehicle trajectories (Xu et al. 2018) are optimised to reduce the computational load. Alternatively, rule-based trajectory planning methods are used to simulate trajectories (Li, Elefteriadou, and Ranka 2014; Yang, Guler, and Menendez 2016). The red indication in (Xu et al. 2018; Feng, Yu, and Liu 2018; Yu et al. 2018) is regarded as terminal condition constraints on the position and/or speed. This unfortunately restricts the applicability on a corridor with multiple intersections, due to the difficulties in determining the terminal conditions at each intersection.

To conclude, current studies are confined to a single subject vehicle as to the trajectory optimisation, excluding the potential benefits of considering the overall platoon. With respect to the signal optimisation, the red phases in existing research of this line are presented by constraining the arrival time and/or terminal conditions, causing additional calculation of arrival time and the restricted application scope of isolated intersections. Therefore, the necessity of proposing an approach to integrating signal optimisation with platoon trajectory planning that is not restricted at isolated intersections arises.

To fill the scientific gaps, this paper proposes an integrated control approach of optimising signals and trajectories for CAV platoons at standard full intersections. In the upper layer, all feasible signal plans are enumerated provided the signal cycle length, and each feasible signal plan is transferred to the lower layer iteratively. The lower layer determines accelerations of the overall CAV platoons under each feasible signal plan, optimising riding comfort (by minimising accelerations) and average travel delay (by maximising speeds), subject to the constraints on admissible accelerations, speed bounds, and safe driving requirements. The red phase is formulated as a logic position constraint so that vehicles can react to signals accordingly. The optimal signal plan is determined in the upper layer by finding the minimal objective function value among all feasible signal plans. The queue discharging and the transmissions from low speeds to high speeds (or vice versa) are taken into account in the lower layer.

The integrated signal and trajectory control approach is flexible owing to the design of the logic red phase constraint. Unlike the existing terminal condition constraints of red phases which require prior knowledge of the arrival time of every vehicle, our formulation applies the logic constraint and thereby is not limited to an isolated intersection. The proposed trajectory optimisation layer can also work under adaptive signals without pre-determining stopping vehicles, which lifts one of the limitations in (Liu, Wang, and Hoogendoorn 2019). The integrated approach is scalable to incorporate different traffic movements during multiple signal phases. Finally, the performance of the integrated control

approach is validated by simulation of three scenarios and two baseline scenarios. Simulation results demonstrate the benefits of the proposed control approach.

The rest of the paper is structured as follows. First, the control architecture is introduced, followed by the integrated control formulation for the vehicle trajectory and the traffic signal. The experiment design and simulation analysis are then discussed. The last section provides conclusions and directions for future work.

2. Control architecture

In this section, the hierarchical control problem is specified, which determines the signal parameters in the upper layer and optimises the vehicle trajectories in the lower layer. Later, the operational assumptions (e.g. minimum and maximum admissible vehicle accelerations) are illustrated.

2.1. Control problem description

Without loss of generality, we consider CAV platoons approach the signalised intersection from four arms, and downstream CAVs are queueing before the stop-lines, as shown in Figure 1 (a). The longitudinal trajectory control algorithm will be triggered when the approaching platoon leader at any direction enters the control zone, which is the interior region of the circle in Figure 1 (a). The centre of the control zone is the signal controller, and the radius of the control zone is the communication range (normally 200 metres).

The control objectives are to determine the optimal signal plan in the upper layer and to optimise accelerations of all CAVs in the lower layer, subject to safety and comfort constraints, as shown in Figure 1 (b). In the upper layer, the feasible signal plans are generated and iteratively imported to the lower layer. In the lower layer, the ride comfort is maximised by minimising accelerations and the travel delay is minimised by maximising vehicle speeds under each iterative signal plan. The control designs of the upper and lower layers are detailed in the forthcoming section.

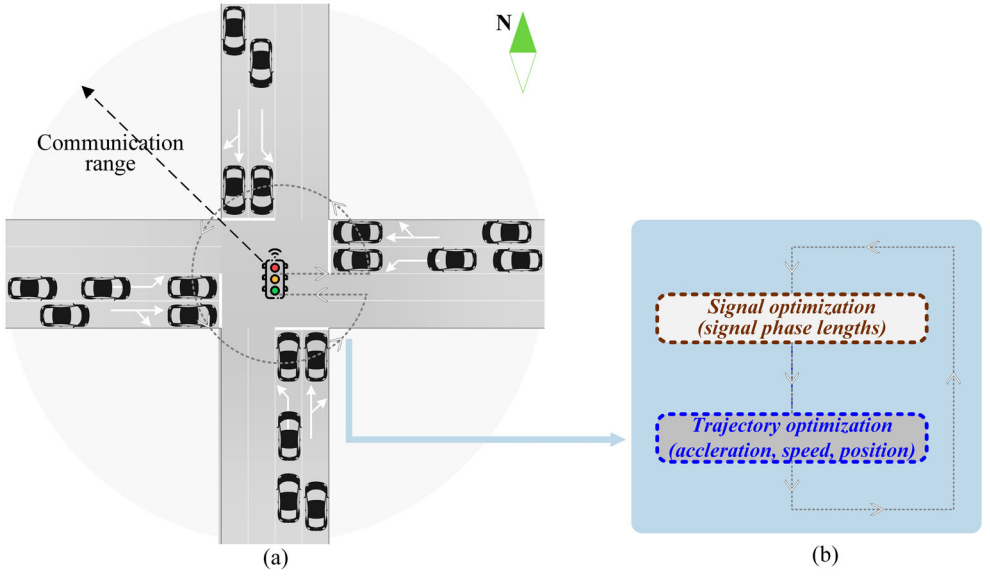

Figure 1. Illustration on Operations of the Control System.

2.2. Design assumptions

The assumptions of the integrated control algorithm are described as follows:

(1) The signal phases are arranged in a predefined sequence at the considered intersection. The phase lengths are controlled under the assumption of a constant cycle length;
(2) All vehicles in the control zone are cooperative and controlled via their accelerations within the admissible range. They exchange position and speed information with each other via V2 V communication;
(3) Signal Phasing and Timing (SPaT) information is delivered to the platoon controller via I2 V communication;
(4) The sum of feedback information and vehicle actuation delay is smaller than 1 s. Hence delays can be omitted in formulation with an acceleration sampling time interval of 1 s.
(5) Lane changing behaviour is not taken into account in the control zone.

Under these assumptions, different geometry configurations of multiple lanes at intersections are able to be accommodated by regarding the traffic movements released during the same green phase but on multiple lanes as multiple platoons of one traffic movement.

3. Control problem formulation

The integrated control problem of trajectories and signals is formulated in this section, including control objectives and constraints, system dynamics, controller formulisation and solution approach.

3.1. Upper layer

Let J denote the total number of green phases for different traffic movements within the signal cycle, and j ($\in J$) is the green phase sequence number in the current cycle. The movement(s) released in the jth green phase refers to the jth movement(s). The yellow change intervals and the all-red clearance time are converted to the effective green and red time. The decision variables in the upper layer are the green phase lengths, g_j, ($j \in J$), the summation of which are equal to the fixed signal cycle length, C:

$$\mathbf{g} = [g_1, g_2, \ldots, g_J]^T \tag{1}$$

$$\sum_{j=1}^{J} g_j = C \tag{2}$$

If $g_j^{\min}$ and $g_j^{\max}$ are the minimal and maximal green time of the jth green phase, then the bounds on green phase lengths are

$$g_j^{\min} \leq g_j \leq g_j^{\max}, \quad \forall j \in J \tag{3}$$

The feasible set of control variables in the upper layer mainly depends on the constraints of green phase lengths. The signal parameters can be optimised based on enumerating the feasible set. Each feasible signal plan is transferred to the lower layer that will determine vehicle trajectories and simultaneously calculate the objective function. The objective function values under all feasible signal plans are recorded and compared to find the optimal signal plan in the upper layer. In other words, the objective functions in the upper and lower layer are the same.

The integration between the upper layer and the lower layer is reflected in the objective function and the constraints. To this end, the upper layer decision variables are conveyed to the lower layer as parameters, which will be detailed in the forthcoming subsection.

3.2. Lower layer

The vehicle trajectories are optimised in the lower layer. The control variable in the lower layer is the acceleration of vehicle i in jth movement, $a_{ij}(t)$, and the state variables are the longitudinal position, $x_{ij}(t)$, and the speed, $v_{ij}(t)$. Here, i denotes the vehicle sequence number and N_j is the total number of controlled vehicles in the jth movement ($1 \leq i \leq N_j$). The control and state variables are defined as:

$$\mathbf{u} = (a_{11}, a_{21}, \ldots, a_{N_1 1}, \ldots, a_{1J}, a_{2J}, \ldots, a_{N_J J})^T \tag{4}$$

$$\mathbf{x} = (\mathbf{x}_{11}, \mathbf{x}_{21}, \ldots, \mathbf{x}_{N_1 1}, \ldots, \mathbf{x}_{1J}, \mathbf{x}_{2J}, \ldots, \mathbf{x}_{N_J J})^T, \quad \mathbf{x}_{ij} = (x_{ij}(t), v_{ij}(t)) \tag{5}$$

The following ordinary differential equation is used to describe the system dynamics model of a single vehicle:

$$\frac{\mathrm{d}}{\mathrm{d}t}\mathbf{x}_{ij} = \frac{\mathrm{d}}{\mathrm{d}t}\begin{pmatrix} x_{ij}(t) \\ v_{ij}(t) \end{pmatrix} = \mathrm{f}(\mathbf{x}_{ij}, \mathbf{u}_{ij}) \tag{6}$$

$$\mathrm{f}(\mathbf{x}_{ij}, \mathbf{u}_{ij}) = A\mathbf{x}_{ij} + B\mathbf{u}_{ij} \tag{7}$$

where

$$A = \begin{bmatrix} 0 & 1 \\ 0 & 0 \end{bmatrix}; \quad B = \begin{bmatrix} 0 \\ 1 \end{bmatrix}$$

If T ($\geq C$) is the prediction horizon, the control problem formulation is described as:

$$f = \min_{\mathbf{u}} \sum_{j=1}^{J} \sum_{i=1}^{N_j} \int_0^T \beta_1 a_{ij}^2(t) - \beta_2 v_{ij}(t)\mathrm{d}t \tag{8}$$

Here, β_1 and β_2 are cost weights. β_1 is unitless and the unit of β_2 is defined as $\mathrm{m/s}^{-3}$. The first cost term in equation (8) is designed to maximise ride comfort by minimising accelerations. The second cost term represents the minimisation of travel delay by maximising speeds.

In addition, the control and state variables are required to obey some constraints in the lower layer, including:

(1) Admissible acceleration

The control variable, acceleration, should be bounded between the maximal acceleration, $a_{\max}$, and the minimal acceleration, $a_{\min}$.

$$a_{\min} \leq a_{ij}(t) \leq a_{\max} \tag{9}$$

(2) Speed bounds

The state variable of speed should be restricted between the limit speed, $v_{\max}$, and 0.

$$0 \leq v_{ij}(t) \leq v_{\max} \tag{10}$$

(3) Safe driving requirements

The following vehicles are required to track the vehicles in front with the safe space and time gaps, which should not be less than the minimum safe gap.

$$x_{ij}(t) - x_{(i+1)j}(t) \geq v_{(i+1)j}(t)t_{\min} + s_0 + l_{ij} \tag{11}$$

Here, l_{ij} denotes the length of vehicle i in the jth movement, $t_{\min}$ is the minimum safe car-following time gap, and s_0 is the minimum space gap at standstill conditions.

(4) Red phase constraint

The red phases can be represented as position constraints in the lower layer. In order to react to the red phase, the logic constraint is applied to generate trajectories facing the signals. Whether vehicles can pass or not is determined by the activation of the logic decision. In this way, the vehicles can be responsive to the adaptive signal changes, without pre-determining the first-stopping vehicle such as the approach in (Liu, Wang, and Hoogendoorn 2019).

Assume the longitudinal position at the stop bar is x_{stop}. If vehicle i in the jth movement cannot pass the intersection during the jth green phase, it cannot leave within the signal cycle either. The red phase is formulated as the logic position constraint, i.e. if the vehicle position at the jth green phase tail is behind the stop-line, the vehicle position at the signal cycle tail is also behind the stop-line.

$$\text{If } x_{ij}\left(\sum_{k=1}^{j} g_j(k)\right) \leq x_{\text{stop}}, \quad \text{then } x_{ij}(C) \leq x_{\text{stop}} \tag{12}$$

Here, k represents the sequence number of green phases no later than the jth green phase.

The lower layer optimisation problem can be solved by applying the upper layer decision variables as parameters. To integrate the lower layer with the upper layer, the lower layer optimisation problem is cast as a constraint to the upper layer optimisation problem.

3.3. Solution approach

The lower layer is a parametric optimisation problem that applies the upper layer decision variables as parameters. Therefore, the upper and lower layers can be integrated by implementing the lower layer optimisation problem as a constraint to the upper layer optimisation problem. As discussed above, the objective function for the upper layer F is the same as the objective function for the lower layer f as in equation (8), thus

$$F = \min_{\mathbf{u}} \sum_{j=1}^{J} \sum_{i=1}^{N_j} \int_0^T \beta_1 a_{ij}^2(t) - \beta_2 v_{ij}(t) \mathrm{d}t \tag{13}$$

The two-layered problem is formulated as follows:

$$\min_{\mathbf{g},\mathbf{u}} F(\mathbf{g}, \mathbf{u}) \tag{14}$$

s.t.

$$\mathbf{u} \in \arg\min_{\mathbf{u}} \{f(\mathbf{g}, \mathbf{u}) : h(\mathbf{g}, \mathbf{u}) \leq 0\} \tag{15}$$

$$G(\mathbf{g}, \mathbf{u}) \leq 0 \tag{16}$$

G and h correspond to the upper layer constraint and the lower layer constraint respectively, i.e. equation (3) and equations (9) to (12). The relationship between the upper layer and the lower layer is depicted in Figure 2, together with the detailed solution approach. In Figure 2 (a), the parametric lower layer optimisation problem can be solved given any upper layer decision vector $\bar{\mathbf{g}}$. Then, the lower layer provides the optimal response considering the lower layer $\bar{\mathbf{u}}^*$ to the upper layer. This parametric flow is defined as an enumeration step of the upper layer.

The solution approach is illustrated in Figure 2 (b). In the upper layer, an enumeration method is adopted to evaluate all feasible signal plans, in other words, to solve the equality constraint of equation (2). Let $\boldsymbol{P}$ denote the upper layer feasible region, i.e. the feasible signal phase lengths. If τ ($\in[1,2,\ldots,\Lambda]$) implies the enumeration step sequence of the upper layer, $\boldsymbol{P}_\tau$ is the feasible signal plan at the τth enumeration step, which is conveyed to the lower layer for trajectory control. The algorithm starts with

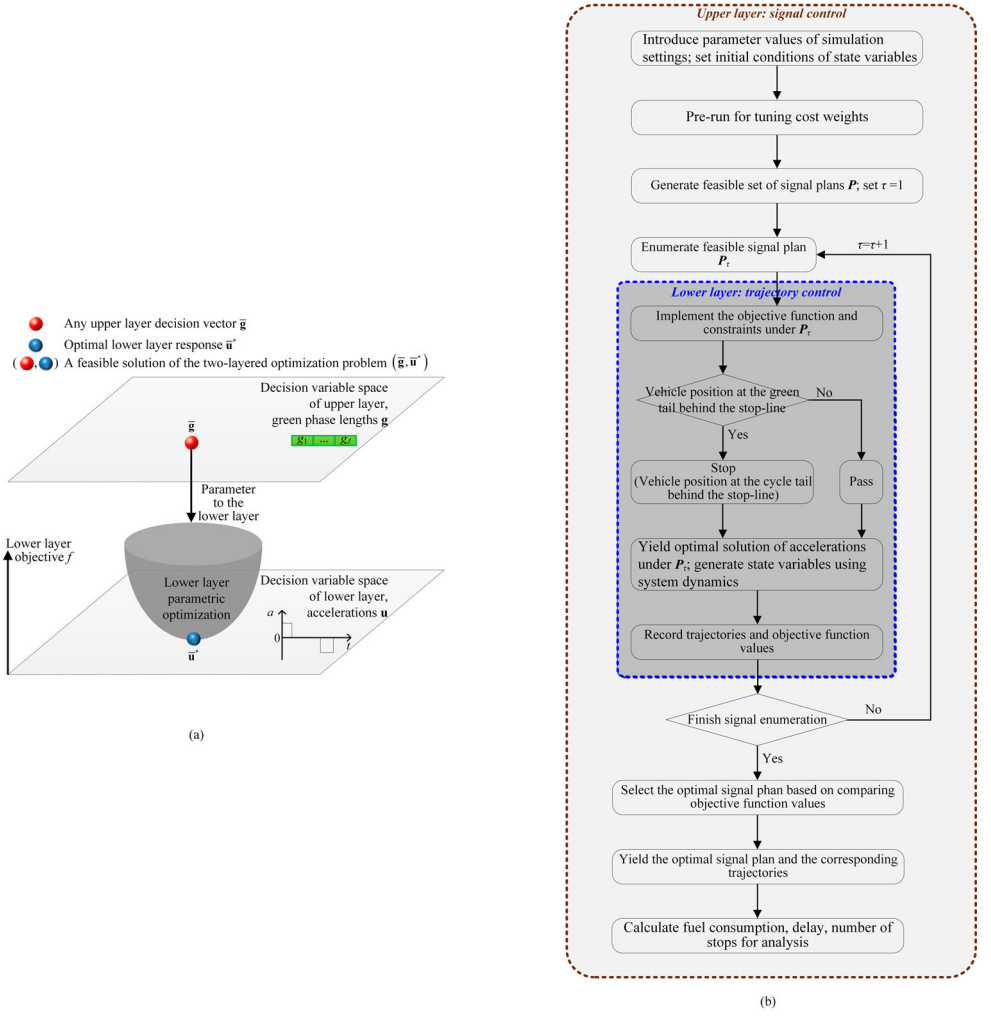

Figure 2. Illustration of the Two-Layered Problem and the Solution Approach.

$\tau = 1$, and then the feasible signal plan $\boldsymbol{P_1}$ is transferred to the lower layer for trajectory optimisation. In the lower layer, the accelerations are optimised and recorded at each enumeration step, together with the corresponding value of the objective function *f*. The enumeration continues ($\tau = \tau + 1$) until all feasible signal plans are evaluated ($\tau = \Lambda$). Finally, the optimal signal plan is selected by comparing values of the objective function in the upper layer *F*. The outputs of the integrated control approach are the optimal signal parameters and the vehicle trajectories.

In the lower layer, the control variable (i.e. acceleration) is discretised in time to solve the continuous-time optimal control problem using nonlinear optimisation techniques (Rao 2009). System dynamics of equation (7) are transformed as linear equality constraints. The control variables, accelerations, are bounded within the admissible range. The linear inequality constraints on state variables, such as the speed bound and the no-collision requirement, are transformed to restrict the control variable using the system dynamics equation. The logic red phase constraint is enforced as the position constraint, under which the vehicles can stop within the cycle if they cannot pass during the green phase, as shown in the diamond of the lower layer in Figure 2 (b). The vehicles are thereby able to react to the instant changes in the phase lengths, which can be applied under adaptive and actuated

signal control approaches. The logic red phase constraint is implemented as nonlinear position constraints for every vehicle. This optimal control problem is solved in MATLAB using fmincon solver. The performance of the controller is simulated and analysed in the following section.

4. Simulation results and analysis

In this section, three scenarios and two baseline scenarios are designed to validate the platoon performance of this control algorithm.

4.1. Experiment design

The vehicle trajectories are simulated at a typical four-arm intersection with three traffic movements while optimising the signal parameters. The left-turn movement is separated from the through and right-turn movements, providing the left-turn exclusive lane and signal phase, while the difference between the right-turn and through movements is ignored. Four signal phases are considered in a signal cycle ($J = 4$). The longitudinal position of the stop-line x_{stop} is set to 0 m. Therefore, the control zone starts from −200 m to 200 m, considering the realistic communication ranges of I2 V and V2 V are about 200 m.

In this experiment settings, the signal cycle length is given ($C = 50$ s) when optimising four green phase lengths ($j = 1, 2, 3, 4$) within the cycle. The prediction horizon T is 60 s, longer than the signal cycle to test the accelerating characteristics of the first movement at the beginning of the subsequent green phase. The time step is 1 s, thus delays under this time step have no effect on trajectories. The initial speed of the approaching vehicles in the first movement is 10 m/s to catch the first green phase ($j = 1$), while the counterparts of other movements are 8 m/s. The various initial speeds are designed to test the feasibility of the control approach under different initial conditions. The signal phase lengths are enumerated from the minimal green phase to the maximal green phase with an increase of 2 s. The choice is motivated by the minimum safe car-following time gap t_{min}, which implies the throughput remains unchanged within 2 s during the green time. Other parameter values are detailed in Table 1, most of which come from the previous work in (Liu, Wang, and Hoogendoorn 2019). Similar settings (e.g. the vehicle number, the green phase number, and signal cycle length) can be simulated in the same way.

In order to test the performance of the integrated control approach, three scenarios and two baseline scenarios are designed. Hereinafter, the symmetric traffic flow refers to the situation that all movements have the same traffic demand level. Otherwise, it is referred to as asymmetric traffic flow. Scenario 1 is designed to validate not only the signal optimisation performance under the symmetric traffic flow but also the platoon characteristics, such as the decelerations of stopping vehicles facing the red phase, the accelerations of passing and queueing vehicles during the green phase. Two queueing vehicles at the stop-line and three approaching vehicles from the boundary of the control zone (−200 m) are set in every direction, thus there are totally 20 vehicles in Scenario 1. Scenario 2 is also simulated under the symmetric traffic flow but one more vehicle is added at the approaching platoon tail, i.e. 24 vehicles in total. The trajectory performance in the approaching platoon and in the queue explores the trajectory pattern of the control approach. Scenario 3 aims to investigate the performance of signal optimisation under the asymmetric traffic flow. The approaching vehicle settings are two vehicles in the first movement, three vehicles in the second movement, four vehicles in the third movement, and five vehicles in the fourth movement, with two vehicles queueing behind the stop bar in every movement. Thus, there are in total 22 vehicles in Scenario 3.

Baseline Scenario 1 has the same settings as Scenario 1, but the vehicles are modelled to represent human driver behaviour. The traffic signals are enumerated and optimised in the same way as Scenario 1 does (using equation (13)), while the trajectories are represented using the intelligent driver model (IDM). The comparisons between Scenario 1 and Baseline Scenario 1 provide insights into the optimal signal pattern of the integrated control approach. In addition, Baseline Scenario 2 has the same

Table 1. Parameter and coefficient values in the experiment.

Notation	Parameter/ Coefficient	Value	Unit
–	time step	1	s
–	initial speed of approaching vehicles	10,8,8,8	m/s
–	initial space gap of approaching vehicles	35	m
–	initial position of the leader in the approaching vehicles	−200	m
–	initial space gap of queueing vehicles	5	m
–	initial position of the leader in the queueing vehicles	−5	m
-	control zone range	200	m
J	green phase number within the signal cycle	4	–
	the maximal green phase	20	s
	the minimal green phase	4	s
C	signal cycle length	50	s
T	prediction horizon length	60	s
x_{stop}	the position of the stop lines at intersections	0	m
l_{ij}	length of vehicle i in the jth movement	3	m
$t_{\min}$	minimum safe car-following time gap	2	s
s_0	minimum space gap at standstill conditions	2	m
$v_{\max}$	limit speed	20	m/s
$a_{\max}$	allowable maximum acceleration	2	m/s^2
$a_{\min}$	allowable minimum acceleration	−5	m/s^2
β_1	cost weight	0.5	–
β_2	cost weight	0.5	m/s^3

Pseudo-code of implementing the simulation experiment

Step 1:	Introduce parameter values of simulation settings [*UP*]
Step 2:	Set initial conditions of state variables [*UP*]
Step 3:	Pre-run for tuning cost weights [*UP*]
Step 4:	Set enumeration step $\tau = 1, \tau \in [1,2,\dots,\Lambda]$ [*UP*]
Step 5:	Generate the feasible set of signal plans $\boldsymbol{P}, \boldsymbol{P_\tau} \in [\boldsymbol{P_1}, \boldsymbol{P_2}, \dots, \boldsymbol{P_\Lambda}]$ [*UP*]
Step 6:	Convey $\boldsymbol{P}$ to the lower layer as parameters [*UP*]
Step 7:	Optimise trajectories under $\boldsymbol{P_\tau}$ [*LW*]
Step 7.1:	**while** $\tau \leq \Lambda$
Step 7.2:	Implement the objective function and constraints under $\boldsymbol{P_\tau}$
Step 7.3:	**if** the vehicle position at the green tail is behind the stop-line $x_{ij}\left(\sum_{k=1}^{j} g_j(k)\right) \leq x_{\text{stop}}$ **then**
Step 7.4:	add constraints on vehicle position at the cycle tail $x_{ij}(C) \leq x_{\text{stop}}$
Step 7.5:	**end**
Step 7.6:	Yield optimal solution of accelerations under $\boldsymbol{P_\tau}$
Step 7.7:	Generate state variables of position and speed using system dynamics
Step 7.8:	Record trajectories and objective function values under $\boldsymbol{P_\tau}$
Step 8:	Select the optimal signal phan by comparing all objective function values under $\boldsymbol{P}$ [*UP*]
Step 9:	Yield the optimal signal plan and the corresponding trajectories [*UP*]
Step 10:	Calculate fuel consumption, delay, number of stops [*UP*]

settings as Scenario 2 but Baseline Scenario 2 only optimises trajectories without signal optimisation. The signal controller is assumed to allocate the green time based on the traffic demand, thus the signal timing plan in Baseline Scenario 2 is 12 s for the first and third movements and 13 s for the second and fourth movements. The comparisons between Scenario 2 and Baseline Scenario 2 can help explore the optimal trajectory pattern. Both the designed scenarios and the baseline scenarios can verify the feasibility of the integrated control approach.

The following pseudo-code shows the implementation of the simulation experiment. UP and LW represent the upper layer and the lower layer respectively. In this simulation, all parameter values and the initial conditions of state variables are first set. Later, the cost weights are tuned under Scenario 1 and then applied in all scenarios. The cost weights of ride comfort and speed, β_1 and β_2, are supposed to keep the same order, thus $\beta_1 = 0.5$ and $\beta_2 = 0.5\,\text{m/s}^3$. The selected cost weights are appropriate to stimulate vehicles for reaching the maximal speed while unnecessary fluctuations in accelerations are avoided. Detailed discussion on tuning cost weights and parameter values can be found in the previous work (Liu, Wang, and Hoogendoorn 2019). Then, the objective function and all linear and

nonlinear constraints are transcribed in the matrix as the fmincon solver required. After optimisation, the optimal solution of acceleration is generated, and thereby the state variables of position and speed can be determined using the system dynamics model. Furthermore, the fuel consumption, delay, and number of stops under all scenarios are calculated to validate the benefits of the integrated control approach. The instantaneous fuel consumption rate f_{eco} (ml/s) could be estimated using

$$f_{\text{eco}} = \begin{cases} b_0 + b_1 v + b_2 v^2 + b_3 v^3 + a(c_0 + c_1 v + c_2 v^2) & a > 0 \\ b_0 + b_1 v + b_2 v^2 + b_3 v^3 & a \leq 0 \end{cases} \tag{17}$$

Here, v and a represent $v_{ij}(t)$ and $a_{ij}(t)$ for simplification. Detailed parameter values can be found in (Kamal et al. 2011).

4.2. Platoon performance

Hereinafter, the designed and baseline scenarios are simulated and analysed to illustrate the control effects. In order to present the trajectories concisely, only the speed and position trajectories are presented, as in Figures 3–6. As shown in these figures, it is evident that all controller constraints are satisfied. The vehicle number N_j, the optimal signal phase lengths, throughputs during the green time, the fuel consumptions, delay, and number of stops are revealed and compared in every scenario, which can further explore the advantages of the proposed control approach. The travel delay is calculated by the vehicle arrival time at the stop-line minus the minimal travelling time to the stop bar, i.e. the distance from the initial position to the stop-line divided by the limit speed $v_{\max}$. These indicators under all scenarios are detailed in Table 2.

4.2.1. Analysis of Scenario 1 and Baseline Scenario 1

The speed trajectories of Scenario 1 and Baseline Scenario 1 are analysed in this subsection, followed by summarising the optimal signal pattern. Finally, the fuel consumptions are calculated and compared.

Speed trajectories of five vehicles per movement are presented under Scenario 1, as shown in Figure 3. The vehicle sequence numbers from 1 to 5 are depicted as V1 to V5 in all subfigures of Figure 3, where V1 and V2 are queueing vehicles (0 speed when $t = 0$ s) and V3 to V5 are approaching vehicles (10 or 8 m/s when $t = 0$ s). As can be seen, the following vehicles always reach the maximal speed later than the predecessors because of the no-collision requirement. The optimal green phase lengths are 6, 13, 13, and 18 s in sequence, releasing 2, 5, 5, and 5 vehicles respectively.

The queueing vehicles in all movements accelerate from standstill conditions at the beginning of the green phases to pass the intersection. In the first movement, as shown in Figure 3 (a), releasing the approaching vehicles will result in wasting the green time, thus the signals are optimised to terminate the first green phase after two queueing vehicles pass the intersection (6 s). The approaching vehicles in the first movement experience stops during the red phase, and start accelerations ($t = 30$ s) to catch the next green phase ($t = 51$ s to $t = 60$ s). In the latter three movements, the approaching vehicles with initial 8 m/s react to the signal changes by accelerating to catch the green phase or decelerating facing the red phase. For instance, the approaching vehicles in the second movement are unnecessary to decelerate owing to the shorter red phase, as shown in Figure 3 (b). In contrast, facing the longer red phase, approaching vehicles in the fourth movement require more decelerations to stop behind the stop bar, as can be seen in Figure 3 (d).

It can be concluded that the safe driving constraints and speed bounds are satisfied in Scenario 1. The red phase constraint is proved to be effective in that all vehicles are able to react to the red phases. The signal parameters are optimised to release as many vehicles as possible thanks to the travel delay cost term. The decelerations of stopping vehicles and the accelerations of passing vehicles are verified to be smooth under Scenario 1.

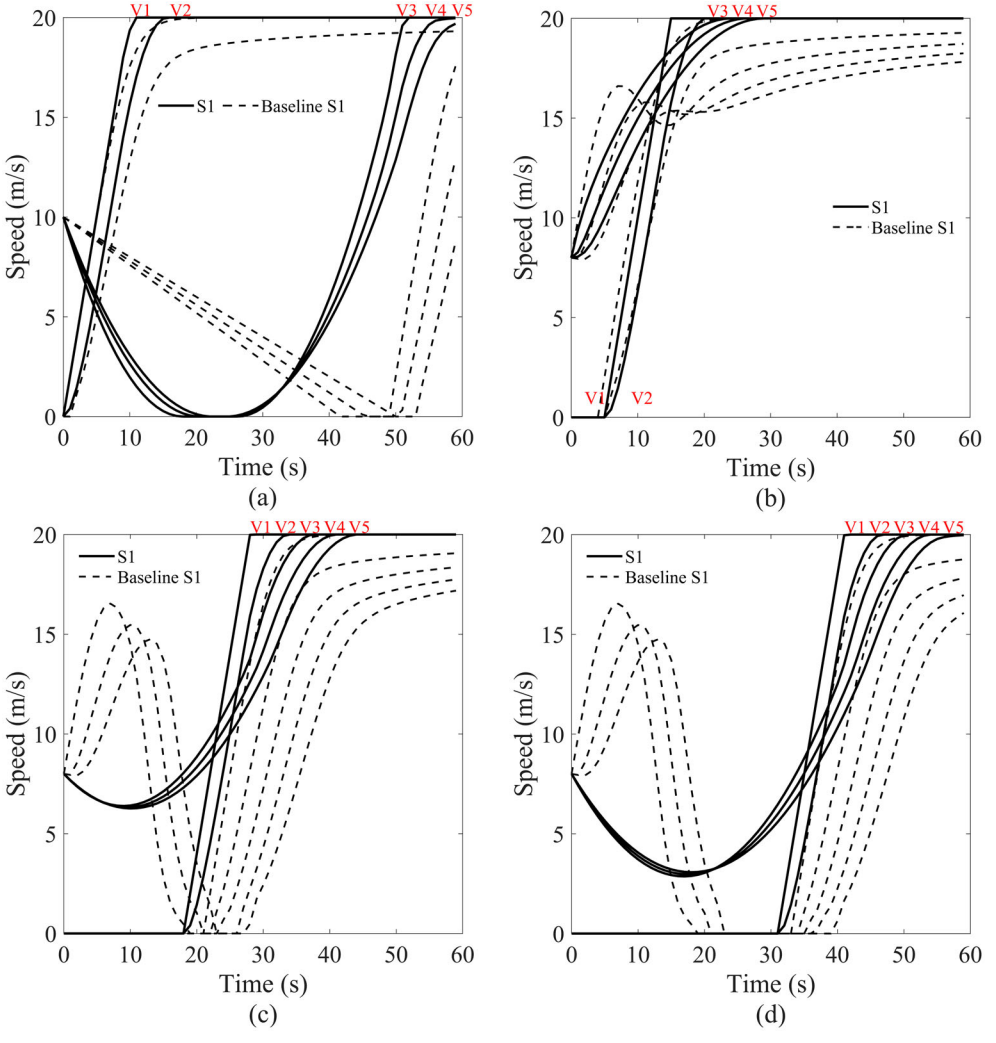

Figure 3. Speed Trajectories under Scenario 1 (S1) and Baseline Scenario 1 (BS1). (a) first movement (b) second movement (c) third movement (d) fourth movement.

Baseline Scenario 1 optimises signals in the same way as Scenario 1 does, based on the trajectories generated by IDM. The red phase is represented using the logic constraint equation (12) when implementing IDM. The speed trajectories of IDM model are illustrated in Figure 3, as depicted in the dashed lines. The green phase lengths are optimised to be 6, 16, 12, and 16 s, and the throughputs are the same as the counterparts in Scenario 1. The signal optimisation also tends to shorten the first green phase to release more vehicles from the latter movements. The latter three green phase lengths are similar between Scenario 1 and Baseline Scenario 1. One reason is that IDM model sometimes fails to operate following vehicles with the maximal speed, which may fluctuate the green phase lengths. Comparing the optimal signal parameters between Scenario 1 and Baseline Scenario 1, the optimal signal pattern can be concluded as switching signal phases in time to release as many vehicles as possible.

In addition, the optimal speeds of the proposed control approach are considerably smooth owing to the ride comfort cost term compared to IDM. Unnecessary accelerations and decelerations during the red time are unavoidable under IDM, causing more fuel consumption. The fuel consumption per metre is calculated according to the instantaneous fuel consumption model in (Kamal et al. 2011) and

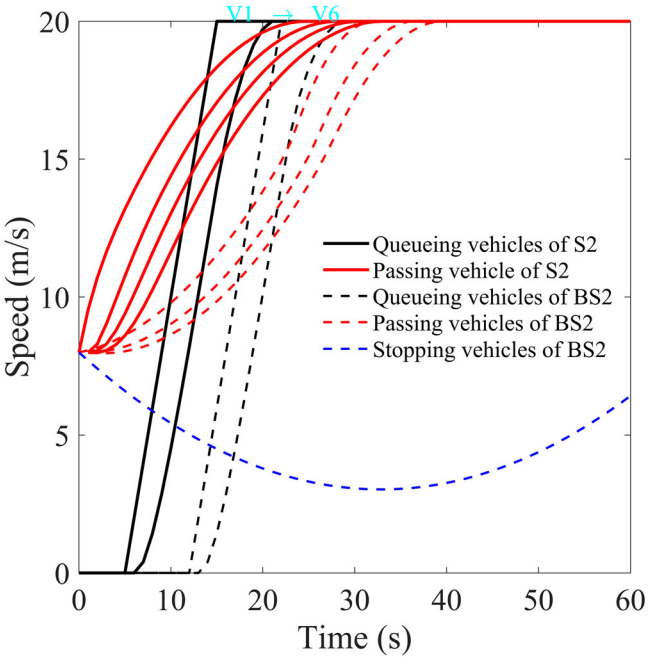

Figure 4. Speed Trajectories of the second movement under Scenario 2 (S2) and Baseline Scenario 2 (BS2).

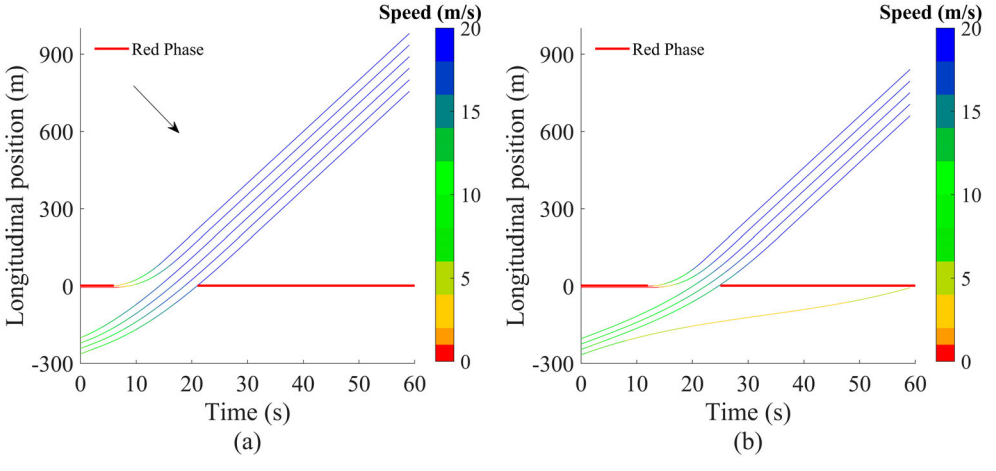

Figure 5. Longitudinal Position of the second movement under Scenario 2 and Baseline Scenario 2. (a) Scenario 2 (b) Baseline Scenario 2.

the travelling distance within the prediction horizon. The integrated approach saves 0.0287 ml/m compared to the IDM model. The minor fuel reduction mainly stems from the speed differences between Scenario 1 and Baseline Scenario 1. The speeds of followers under Baseline Scenario 1 are difficult to reach the maximal speed, which also deteriorates the traffic delay. This can also be seen in the objective function values, 7227.7 in Scenario 1 and 6234.4 in Baseline Scenario 1. Although the advantages of the integrated control approach on fuel efficiency and traffic delay are inconspicuous under Scenario 1, the different numbers of vehicle stops distinguish the benefits of the integrated control approach on trajectory optimisation.

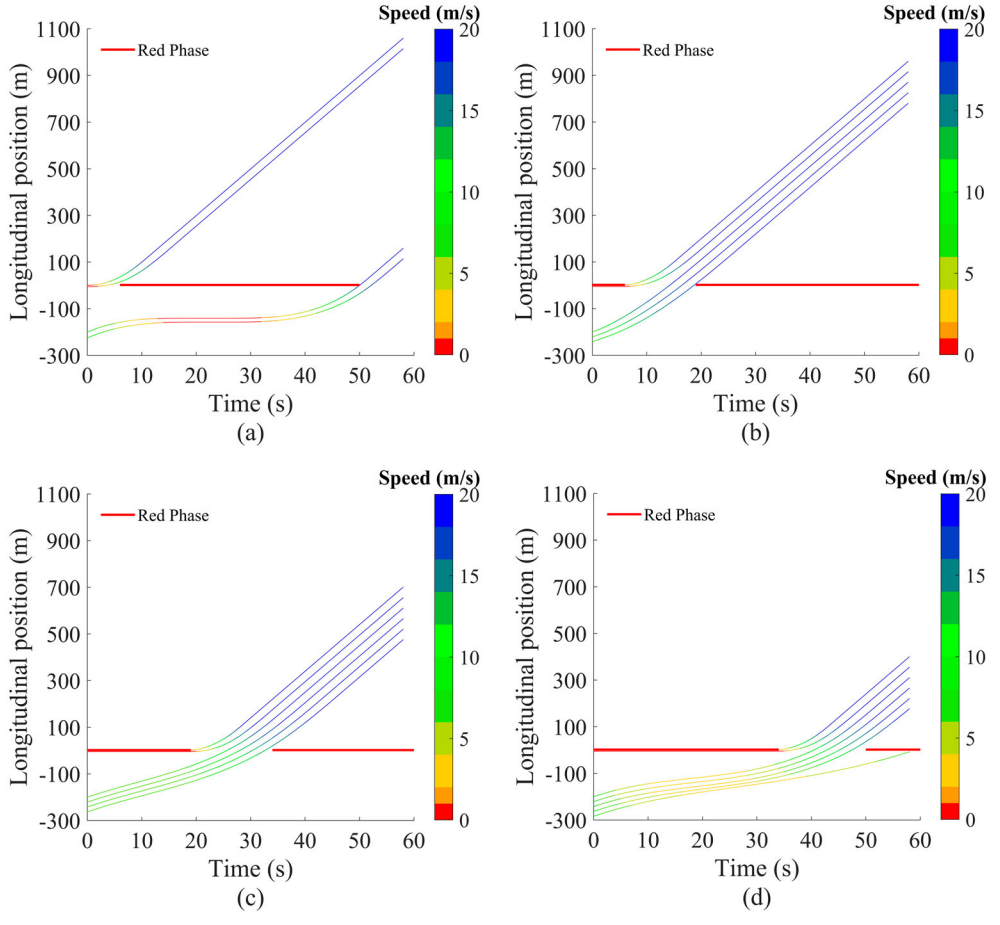

Figure 6. Longitudinal Position under Scenario 3. (a) first movement (b) second movement (c) third movement (d) fourth movement.

Table 2. Indicators under all scenarios.

Indicators/Scenarios	Scenario 1	Scenario 2	Scenario 3	Baseline Scenario 1	Baseline Scenario 2
Vehicle number of the jth ($j = 1,2,3,4$) movement, N_j (veh)	5, 5, 5, 5	6, 6, 6, 6	4, 5, 6, 7	5, 5, 5, 5	6, 6, 6, 6
Optimal/ Pre-timed green phase lengths of the jth ($j = 1,2,3,4$) movement	6, 13, 13, 18	6, 15, 15, 14	6, 13, 15, 16	6, 16, 12, 16	12, 13, 12, 13
Throughputs of the jth ($j = 1,2,3,4$) movement (veh)	2, 5, 5, 5	2, 6, 6, 5	2, 5, 6, 6	2, 5, 5, 5	2, 5, 5, 5
Fuel consumptions (ml/m)	0.0804	0.0837	0.0841	0.1091	0.0830
Objective function value (m^2/s^4)	7227.7	8093.6	7719.1	6234.4	7130.7
Number of stops	3	4	2	9	4
Delay (s)	21.49	24.36	22.76	23.29	29.32

4.2.2. Analysis of Scenario 2 and Baseline Scenario 2

Hereinafter, the speed and position trajectories of the second movement are presented under Scenario 2 and Baseline Scenario 2. The optimal trajectory pattern is concluded in this subsection. Finally, the fuel consumptions are evaluated.

Scenario 2 introduces one more vehicle at the platoon tail in every movement, including two queueing vehicles and four approaching vehicles per movement. For concise illustration, the second

movement is selected to demonstrate the performance, as in Figures 4 and 5. Other movements have similar trajectories.

As shown in Figure 4, the approaching vehicles V3 to V6 (as shown in red lines) climb to the maximal speed over time, but later than the queueing vehicles V1 and V2 as depicted in black lines. The speed trajectories under Scenario 2 in Figure 4 have similar features as under Scenario 1 in Figure 3 (b). The optimal green phase lengths under Scenario 2 are 6, 15, 15, and 14 s, with 2, 6, 6, and 5 vehicles passing the intersection respectively. The trajectories in Figures 4 and 5 prove that the safe following requirement, the speed bounds, and the red phase constraint are respected.

The first green phase length is 6 s, switching signals after releasing the queueing vehicles in the first movement. However, the second and third green phases are longer than the counterparts under Scenario 1, because one more vehicle is optimised to depart the intersection. The last vehicle in the fourth movement cannot pass for lack of green time. Compared to Scenario 1, two more vehicles are released in Scenario 2 considering the same cycle length, which explores the benefits of signal optimisation in the upper layer.

Baseline Scenario 2 (the same settings as Scenario 2) optimises the trajectories individually under the fixed timing plan, other than the cooperative optimisation of four movements in Scenario 2. In Baseline Scenario 2, two vehicles, five vehicles, five vehicles, and five vehicles are optimised to depart the intersection in sequence. The passing vehicles and the signal indication in the second movement can be seen in Figure 5 (b). Figures 4 and 5 show that all constraints in the lower layer are satisfied.

The throughputs in Scenario 2 outperform the counterparts in Baseline Scenario 2, especially in the second and third movements. On one hand, the green time allocation under fixed timing probably causes the waste of green time. On the other hand, throughput is implicitly optimised in the upper layer of the integrated control approach, because the feasible signal plans of releasing fewer vehicles are abandoned owing to the travel delay cost term.

The optimal trajectories in Scenario 1 are similar to Scenario 2. The optimal trajectory pattern can be summarised into three categories based on Scenario 1, Scenario 2, and Baseline Scenario 2, as shown in Figures 3–5. First, the queueing vehicles accelerate from the stationary condition at the beginning of the green phase, trying to reach the maximal speed as soon as possible. The second category refers to the passing vehicles, normally the first several vehicles in the approaching platoon. If facing a shorter red phase, such as in the second movement, they are optimised to accelerate but slower than the queueing vehicles to keep the safe gaps with the preceding vehicles. If facing a longer red phase, such as in the third or fourth movement, they decelerate first and then accelerate smoothly to avoid stops and arrive at the stop-line with higher speeds. The third category contains the stopping vehicles, normally the last several vehicles in the approaching platoon. They decelerate smoothly within the current cycle, and then accelerate to pass the intersection with larger speeds during the next green phase.

As shown in the red lines and red dashed lines in Figure 4, the speed trajectories of passing vehicles in the second movement are presented. The various speed trajectories result from the different optimal lengths of the first green phase between Scenario 2 and Baseline Scenario 2, but both speed trajectories respect the optimal trajectory pattern. The passing vehicles in Scenario 2 accelerate quickly facing a shorter red phase (6 s). And the counterparts of red dashed lines under Baseline Scenario 2 face a longer red phase (12 s), so they accelerate slowly during the red phase in order to keep the safe gap with the queueing vehicles, and then climb to the maximal speed after merging with the queueing vehicles during the green phase. The trajectory difference in other movements between Scenario 2 and Baseline Scenario 2 is negligible.

The fuel consumptions per metre under Scenario 2 and Baseline Scenario 2 are almost identical, as shown in Table 2. However, the total fuel consumptions of all vehicles by integrating fuel consumption rates in time are different, 1370.1 ml in Scenario 2 and 1155.7 ml in Baseline Scenario 2, because more vehicles are released in Scenario 2. The same reason holds for the different objective function values, i.e. 8093.6 in Scenario 2 and 7130.7 in Baseline Scenario 2. In addition, the calculation of travel delay

proves that more travel time is saved under Scenario 2, which demonstrates the superiority of the integrated control approach on signal optimisation.

4.2.3. Analysis of Scenario 3

In Scenario 3, 22 vehicles are simulated under the asymmetric traffic flow. The signals are optimised as 6, 13, 15, and 16 s respectively, and 2, 5, 6, and 6 vehicles depart the signalised intersection. The signal optimisation tends to shorten the first green phase for releasing as many vehicles as possible in the latter movements, as concluded in the analysis of the signal pattern. In addition, it is verified that signal optimisation can react to different traffic demand levels, switching signals for optimal performance. The trajectory performance in Scenario 3 also obeys the optimal trajectory pattern, as discussed in the analysis of Scenario 2. The longitudinal positions in all movements are depicted in Figure 6, with the red lines indicating the optimal signal plan. The fuel consumptions per metre under Scenario 3 is 0.0841 ml/m.

5. Conclusions and future work

In this paper, we proposed an integrated approach for controlling traffic signals and vehicles trajectories at intersections. The problem is formulated as a two-layered optimisation model. The upper layer enumerates all feasible signal plans and sends them to the lower layer iteratively. The lower layer determines the accelerations of the overall platoons at each enumeration step, until completing the signal enumeration. The riding comfort and average travel delay are optimised, subject to safe and physical constraints. To be noted, the red phase is represented using the logic constraint, which enables vehicles to respond to the adaptive signal indication. The upper layer finds the optimal signal plan after enumeration, by searching the minimal objective function value among all enumeration steps. The proposed control approach is feasible in incorporating multiple traffic movements and signal phases, and the benefits of optimising the overall platoon are taken into account. Simulation under three scenarios and two baseline scenarios demonstrated the performance of the approach.

The simulation results show the potentials of throughput improvement and environmental benefits. Based on analysing the performance of all scenarios, the optimal signal pattern and the optimal trajectory pattern are revealed.

The enumeration method in the signal optimisation layer results in intensive computational time, which requires further improvement. Future research is directed to relieve computational load and include the mixed traffic flow of human drivers and CAVs.

Disclosure statement

No potential conflict of interest was reported by the author(s).

Funding

This work was supported by China Scholarship Council: [Grant Number No. 201706320313].

ORCID

J. Zhao http://orcid.org/0000-0003-0741-4911
S. P. Hoogendoorn http://orcid.org/0000-0002-1579-1939

References

Ahmane, M., A. Abbas-Turki, F. Perronnet, J. Wu, A. El Moudni, J. Buisson, and R. Zeo. 2013. "Modeling and Controlling an Isolated Urban Intersection Based on Cooperative Vehicles." *Transportation Research Part C: Emerging Technologies* 28: 44–62.

Altan, O. D., G. Wu, M. J. Barth, K. Boriboonsomsin, and J. A. Stark. 2017. "Glidepath: Eco-Friendly Automated Approach and Departure at Signalized Intersections." *IEEE Transactions on Intelligent Vehicles* 2 (4): 266–277.

Asadi, B., and A. Vahidi. 2010. "Predictive Cruise Control: Utilizing Upcoming Traffic Signal Information for Improving Fuel Economy and Reducing Trip Time." *IEEE Transactions on Control Systems Technology* 19 (3): 707–714.

Feng, Y., C. Yu, and H. X. Liu. 2018. "Spatiotemporal Intersection Control in a Connected and Automated Vehicle Environment." *Transportation Research Part C: Emerging Technologies* 89: 364–383.

Guler, S. I., M. Menendez, and L. Meier. 2014. "Using Connected Vehicle Technology to Improve the Efficiency of Intersections." *Transportation Research Part C: Emerging Technologies* 46: 121–131.

Guo, Y., J. Ma, C. Xiong, X. Li, F. Zhou, and W. Hao. 2019. "Joint Optimization of Vehicle Trajectories and Intersection Controllers with Connected Automated Vehicles: Combined Dynamic Programming and Shooting Heuristic Approach." *Transportation Research Part C: Emerging Technologies* 98: 54–72.

Hao, P., G. Wu, K. Boriboonsomsin, and M. J. Barth. 2018. "Eco-Approach and Departure (EAD) Application for Actuated Signals in Real-World Traffic." *IEEE Transactions on Intelligent Transportation Systems* 99 (99): 1–11.

He, X., H. X. Liu, and X. Liu. 2015. "Optimal Vehicle Speed Trajectory on a Signalized Arterial with Consideration of Queue." *Transportation Research Part C: Emerging Technologies* 61: 106–120.

HomChaudhuri, B., A. Vahidi, and P. Pisu. 2017. "Fast Model Predictive Control-Based Fuel Efficient Control Strategy for a Group of Connected Vehicles in Urban Road Conditions." *IEEE Transactions on Control Systems Technology* 25 (2): 760–767.

Jiang, H., J. Hu, S. An, M. Wang, and B. B. Park. 2017. "Eco Approaching at an Isolated Signalized Intersection Under Partially Connected and Automated Vehicles Environment." *Transportation Research Part C: Emerging Technologies* 79: 290–307.

Kamal, M. A. S., M. Mukai, J. Murata, and T. Kawabe. 2011. "Ecological Vehicle Control on Roads with up-Down Slopes." *IEEE Transactions on Intelligent Transportation Systems* 12 (3): 783–794.

Kamal, M. A. S., M. Mukai, J. Murata, and T. Kawabe. 2012. "Model Predictive Control of Vehicles on Urban Roads for Improved Fuel Economy." *IEEE Transactions on Control Systems Technology* 21 (3): 831–841.

Lee, J., and B. Park. 2012. "Development and Evaluation of a Cooperative Vehicle Intersection Control Algorithm Under the Connected Vehicles Environment." *IEEE Transactions on Intelligent Transportation Systems* 13 (1): 81–90.

Lee, J., B. Park, and I. Yun. 2013. "Cumulative Travel-Time Responsive Real-Time Intersection Control Algorithm in the Connected Vehicle Environment." *Journal of Transportation Engineering* 139 (10): 1020–1029.

Li, J., M. Dridi, and A. El-Moudni. 2014a. "Multi-Vehicles Green Light Optimal Speed Advisory Based on the Augmented Lagrangian Genetic Algorithm." Paper presented at the 17th international IEEE conference on Intelligent Transportation Systems (ITSC), Qingdao, China.

Li, Z., L. Elefteriadou, and S. Ranka. 2014b. "Signal Control Optimization for Automated Vehicles at Isolated Signalized Intersections." *Transportation Research Part C: Emerging Technologies* 49: 1–18.

Liu, M., M. Wang, and S. Hoogendoorn. 2019. "Optimal Platoon Trajectory Planning Approach at Arterials." *Transportation Research Record: Journal of the Transportation Research Board* 2673 (9): 214–226.

Rao, A. V. 2009. "A Survey of Numerical Methods for Optimal Control." *Advances in the Astronautical Sciences* 135 (1): 497–528.

Stebbins, S., M. Hickman, J. Kim, and H. L. Vu. 2017. "Characterising Green Light Optimal Speed Advisory Trajectories for Platoon-Based Optimisation." *Transportation Research Part C: Emerging Technologies* 82: 43–62.

Stevanovic, A., J. Stevanovic, and C. Kergaye. 2013. "Green Light Optimized Speed Advisory Systems: Impact of Signal Phasing Information Accuracy." *Transportation Research Record: Journal of the Transportation Research Board* 2390 (1): 53–59.

Ubiergo, G. A., and W. Jin. 2016. "Mobility and Environment Improvement of Signalized Networks Through Vehicle-to-Infrastructure (V2I) Communications." *Transportation Research Part C: Emerging Technologies* 68: 70–82.

Wan, N., A. Vahidi, and A. Luckow. 2016. "Optimal Speed Advisory for Connected Vehicles in Arterial Roads and the Impact on Mixed Traffic." *Transportation Research Part C: Emerging Technologies* 69 (2016): 548–563.

Wang, M., W. Daamen, S. Hoogendoorn, and B. Van Arem. 2014. "Potential Impacts of Ecological Adaptive Cruise Control Systems on Traffic and Environment." *IET Intelligent Transport Systems* 8 (2): 77–86.

Wang, Z., G. Wu, and M. J. Barth. 2019. "Cooperative Eco-Driving at Signalized Intersections in a Partially Connected and Automated Vehicle Environment." *IEEE Transactions on Intelligent Transportation Systems* 1 (1): 1–10.

Xu, B., X. J. Ban, Y. Bian, W. Li, J. Wang, S. E. Li, and K. Li. 2018. "Cooperative Method of Traffic Signal Optimization and Speed Control of Connected Vehicles at Isolated Intersections." *IEEE Transactions on Intelligent Transportation Systems* 20 (99): 1–14.

Yang, K., S. I. Guler, and M. Menendez. 2016. "Isolated Intersection Control for Various Levels of Vehicle Technology: Conventional, Connected, and Automated Vehicles." *Transportation Research Part C: Emerging Technologies* 72: 109–129.

Yu, C., Y. Feng, H. X. Liu, W. Ma, and X. Yang. 2018. "Integrated Optimization of Traffic Signals and Vehicle Trajectories at Isolated Urban Intersections." *Transportation Research Part B: Methodological* 112 (2018): 89–112.

Yu, C., W. Sun, H. X. Liu, and X. Yang. 2019. "Managing Connected and Automated Vehicles at Isolated Intersections: From Reservation- to Optimization-Based Methods." *Transportation Research Part B: Methodological* 122 (2019): 416–435.

Zhao, J., V. L. Knoop, and M. Wang. 2020. "Two-Dimensional Vehicular Movement Modelling at Intersections Based on Optimal Control." *Transportation Research Part B: Methodological* 138: 1–22.

Zhao, W., D. Ngoduy, S. Shepherd, R. Liu, and M. Papageorgiou. 2018. "A Platoon Based Cooperative Eco-Driving Model for Mixed Automated and Human-Driven Vehicles at a Signalised Intersection." *Transportation Research Part C: Emerging Technologies* 95: 802–821.

Zohdy, I. H., and H. A. Rakha. 2016. "Intersection Management Via Vehicle Connectivity: The Intersection Cooperative Adaptive Cruise Control System Concept." *Journal of Intelligent Transportation Systems* 20 (1): 17–32.